Materials Science & Engineering C 113 (2020) 110913

Contents lists available at ScienceDirect

Materials Science & Engineering C

journal homepage: www.elsevier.com/locate/msec

Construction of 3D fibrous PCL scaffolds by coaxial electrospinning for protein delivery

Mehrnoosh Rafiei[a], Elaheh Jooybar[a], Mohammad J. Abdekhodaie[a,*], Mansour Alvi[b]

[a] Department of Chemical and Petroleum Engineering, Sharif University of Technology, Tehran, Iran
[b] Athlete's Care Sports Medicine Centre, Toronto, Canada

ARTICLE INFO

Keywords:
Wet electrospinning
3D porous PCL scaffold
Core-shell fibers
BSA sustained release

ABSTRACT

In this study, a three-dimensional tablet-like porous scaffold, comprising core-shell fibers to host proteins inside the core, was developed. The fabrication method involved the novel combination of coaxial and wet electrospinning in a single setting. Poly (ε-caprolactone) was chosen as the based polymer and bovine serum albumin was used as a model protein. These 3D tablet-like scaffolds exhibited adequate porosity and suitable pore size for cell culture and cell infiltration, in addition to appropriate mechanical properties for cartilage tissue engineering. The effects of different parameters on the behavior of the system have been studied and the 3D scaffold based on the core-shell fiber was compared with that based on the matrix fiber. The core-shell structure showed superior performance in comparison to the matrix structure by sustaining protein release kinetics at least for 12 days in PBS. The results from in vitro cell cytotoxicity study revealed that the presented scaffold was biocompatible and non-toxic. Coaxial electrospinning was shown to be a versatile technique in achieving the delivery of biochemical signals in a controlled manner for the regeneration of cartilage. These 3D tablet-like PCL scaffolds incorporated with protein solutions are engineered systems that closely mimic the characteristics of cartilage tissue.

1. Introduction

Aging, trauma, and developmental disorders are the factors that cause cartilage defects, joint pain and loss of mobility. Current treatment strategies are inadequate in restoring the hyaline cartilage function and providing long-term rehabilitation. Tissue engineering holds promise to construct engineered scaffolds which would restore optimal function of the tissue and simultaneously regenerate the damage by hosting cells and signaling molecules [1–6]. Among vast methods of constructing scaffolds, the electrospinning method remains as a simple means to produce scaffolds of ultra-fine fibers using a variety of biodegradable polymers. Fibrous scaffolds constructed by electrospinning, with the advantage of structural harmony with natural extracellular matrix (ECM), may be a viable option for tissue engineering applications.

The electrospinning method was started by using single-fluid flow [7]. Then, more complicated spinning methods were pursued using two or multi-component materials. In this regard, coaxial [8] and modified coaxial [9] spinning methods were developed to provide diverse fiber compositions. Side-by-side [10] spinning method was also introduced to fabricate two component fibers. Unlike coaxial spinning, in this method the polymer solutions are spun from two different nozzles, which are place side-by-side. Therefore, both fiber components have equal exposure on the surface. Other electrospinning methods for fabrication of multilayered nano and microfibers are tri-axial [11] and modified tri-axial [12] and multiple-fluid processes [13] that are used for special applications.

The major drawback of traditional electrospinning method in tissue engineering is the two-dimensional structure of the fibers and inherent low porosity of scaffolds that limit cell seeding, attachment and infiltration. To overcome this issue, researchers have adopted new techniques, such as using special collectors [14,15]; wet electrospinning or by employing porogen particles, which are chemical blowing agents incorporated in the core of the fibers [14]. Wet electrospinning was first introduced by Yokoyama et al. [16] for the lab-scale production of fibrous scaffolds for tissue engineering. Wet electrospinning is a simple and effective method to produce three-dimensional (3D) sponge-like constructs, eliminating the need for complex devices or special chemical additives. In this method, the conventional metallic collector is replaced with a liquid one. In this process, the threads are submerged in a chemical bath that is a non-solvent for the polymer which is compatible with the solvent used in the polymer solution [17].

* Corresponding author.
E-mail address: abdmj@sharif.edu (M.J. Abdekhodaie).

https://doi.org/10.1016/j.msec.2020.110913
Received 22 May 2018; Received in revised form 14 March 2020; Accepted 31 March 2020
Available online 01 April 2020
0928-4931/

Electrospun scaffolds also have the potential application for an effective drug delivery system by virtue of the porous structure and the concomitant large specific surface area [6,14,15]. In pursuit of improving electrospun scaffolds' biological functionality, special biomolecules may be incorporated, either during or after completion of the electrospinning process. Direct inclusion of the biomolecules, generally is achieved by two different approaches: blend electrospinning and coaxial electrospinning. Coaxial electrospinning was developed later that can produce fibers with different type of structures including core-shell, nano coating and monolithic as well [18]. Drugs, proteins and even DNA could be incorporated in the core solution to be protected from harmful solvents of polymer solution, in addition to establishing a controlled release regime.

So far, several efforts have been undertaken for acquiring the methodology of preparing protein-loaded electrospun scaffolds, applying these two techniques. Although previous studies have provided different protein release profiles from blend [17,19–21] and coaxial fibers [19,22–29], limited attention has been paid to comparing them in terms of sustainability to determine which method provides a more controllable system for biomolecule release from electrospun scaffolds.

The aim of the present study is to construct poly (caprolactone)-based 3D scaffolds incorporating biomolecules via either using the blend electrospinning or utilization of coaxial electrospinning technique. In essence, a 3D electrospun PCL scaffold was fabricated and characterized by high porosity and suitable mechanical properties, which is expected to enhance cell attachment and proliferation. Moreover, release kinetics of the loaded bovine serum albumin (BSA), as a model protein, for the two systems were compared.

2. Materials and methods

2.1. Materials

Poly (ε-caprolactone) (PCL,M_n = 80,000) and BSA were purchased from Sigma-Aldrich. Coomassie Brilliant Blue G-250 and organic solvents chloroform and dimethylformamide (DMF) were supplied by Merck chemicals. Dulbecco's Modified Eagle Medium (DMEM), fetal bovine serum (FBS), penicillin, and streptomycin were purchased from Gibco. 3-[4,5-dimethylthiazol-2-yl]-2,5-diphenyl tetrazolium bromide (MTT) was obtained from Sigma-Aldrich. All other chemicals were analytical grade and used as received.

2.2. Fabrication of 3D core-shell fibrous scaffolds

To analyze the effect of different parameters and characterization of scaffolds, 7 different types of scaffolds were prepared by either blend or coaxial electrospinning; the processing parameters and electrospinning methods for each scaffold are listed in Table 1. A coaxial wet electrospinning system was used to fabricate the 3-D fibrous scaffolds, which is schematically illustrated in Fig. 1. It consisted of vertical syringes equipped with a coaxial metal needle that was connected to a positive, high voltage source and a liquid collector basin with an electrically grounded metal plate placed inside. A glass bath filled with the mixture of distilled water and ethanol (1:9 v/v) was used. The selected spinneret was a coaxial needle of 14 and 16 gauges (G) caliber for the shell and core solutions, respectively. BSA was dissolved in distilled water (10 mg/ml) as the core solution. The shell solution was prepared by dissolving Poly (ε-caprolactone) in chloroform: DMF solution (70:30 (v/v)). To study the effect of flow rate ratios between the shell and core solution, the ratios of 3:1 and 3:0.5 were fabricated. The optimum flow rate ratio between the shell and core solutions was 3:1 with feeding velocity of the shell at 3 ml/h rate. The voltage gradient was adjusted between 7 and 12 kV. The distance between tip and the liquid surface was fixed at 7 cm and the pool depth was set at 3 cm.

To have scaffolds with the same amount of loaded protein, 100 μl of BSA solution (10 mg/ml) was spun in each experiment. In this way, the theoretical amount of encapsulated BSA was 1 mg in each scaffold. Afterwards, the samples were rinsed with ethanol for 15 min and then immediately were pressed with a single punch tablet press matrix that was 1 cm in diameter. The fibers were compressed to reach the predetermined density and porosity. The tablet-like samples were dried in a vacuum oven for 3 days at thermostatic room temperature (24 °C) (Fig. 2).

Table 1
Experimental groups and sample preparation at 7–11 kV voltage.

Sample	Preparation method	Polymer solution	Flow rate (ml/h)
1-BSA	Blend Electrospinning	10% w/v PCL/CF & DMF + 2% w/w BSA/Total mass	3
2-BSA	Blend Electrospinning	12% w/v PCL/CF and DMF + 2% w/w BSA/Total mass	3
3-BSA	Blend Electrospinning	15% w/v PCL/CF and DMF + 2% w/w BSA/Total mass	3
4-BSA	Coaxial Electrospinning	Shell: 10% w/v PCL/CF&DMF Core: 1% w/v BSA/DI water	Shell: 3; core:1
5-BSA	Coaxial Electrospinning	Shell: 12% w/v PCL/CF&DMF Core: 1% w/v BSA/DI water	Shell: 3; core:1
6-BSA	Coaxial Electrospinning	Shell: 15% w/v PCL/CF&DMF Core: 1% w/v BSA/DI water	Shell: 3; core:1
7-BSA	Coaxial Electrospinning	Shell: 15% w/v PCL/CF&DMF Core: 1% w/v BSA/DI water	Shell: 3; core:0.5

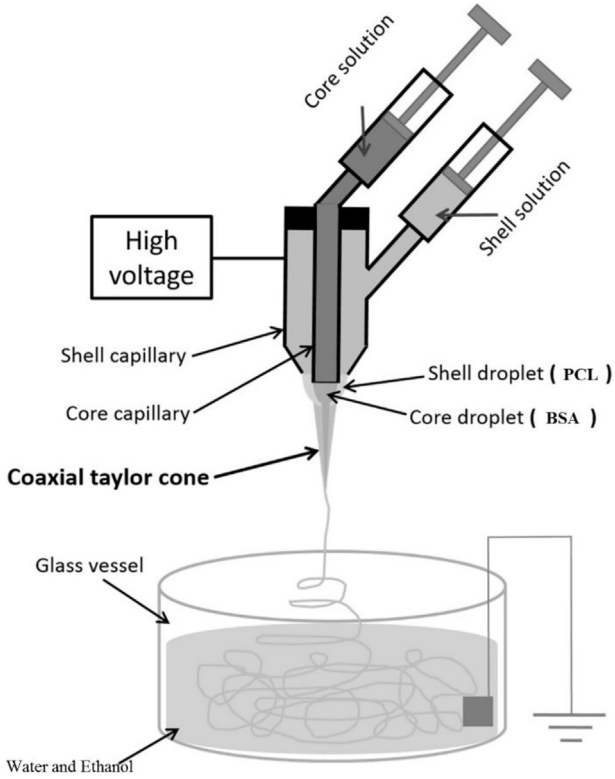

Fig. 1. Schematic representation of coaxial wet electrospinning.

2.3. Morphological characterization of electrospun scaffolds

2.3.1. Scanning electron microscopy (SEM)

Each scaffold was frozen in liquid nitrogen and cut uniformly into thin film specimens. The morphologies of the electrospun fibers were examined using scanning electron microscopy (SEM) at an accelerating voltage of 15 kV. Prior to SEM examination, the films were sputter-coated with gold. The average size of the structural components (fiber diameter, porosity, etc.) was measured and reported using SEM images

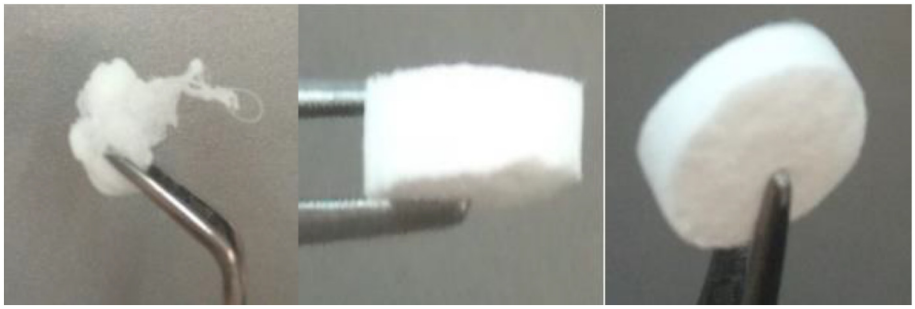

Fig. 2. Fabricated 3D scaffolds before (left) and after molding (right).

by analyzing > 40 fibers. The fibers were analyzed using Image J software. Each test was done at least 3 times.

2.3.2. Transmission electron microscopy (TEM)

The core–shell structure was verified by transmission electron microscopy (TEM). The fiber structure of the coaxial scaffolds incorporating BSA was examined using a 'Philips cm300' transmission electron microscope, operated at 200 kV. The samples for TEM were prepared by direct deposition of the electrospun 2-D fibers onto Formvar carbon films on copper grids.

2.3.3. Porosity of the scaffolds

Scaffold porosity was determined by gravimetric method. This method is simple and fast with common errors based on actual volume measurements of scaffold which preferred for materials that cannot withstand the high pressures used in other porosity determination methods such as layers of nanofiber mats [30]. Scaffold porosity (ε) was calculated using following equations [31–33]:

$$\rho = \frac{m(g)}{A(cm^2) \times h(cm)} \quad (1)$$

$$\varepsilon = \left(1 - \frac{\rho}{\rho_0}\right) \times 100 \quad (2)$$

where, ρ is the apparent density, m is the mass of the dried scaffold, A is the area of scaffold, h is the thickness of scaffold, and ρ_0 is the bulk density of the scaffold. For this study, three samples of 6-BSA scaffold with different apparent densities were selected and molded in a fix mold with constant shape and diameter. Then, scaffolds with a diameter of 10 mm were obtained. The scaffold's thickness was also measured with a micrometer and the volume was calculated by measuring the length, width, and height of the sample. After measuring the scaffold's weight, the apparent density was calculated from Eq. (1). To calculate the porosity, Eq. (2) was used, where ρ_0 is 1.145 g/cm^3.

2.4. In vitro BSA release

To determine the BSA release profile from the loaded scaffold, each sample (with 45 mg weight) were placed in each well of a 12-well tissue culture plate and immersed in 4.0 ml of 0.1 M phosphate-buffered saline (PBS, pH 7.4). These plates were placed in a shaker incubator (37 °C, 70 rpm). At predetermined time intervals, 1 ml of release medium was collected and replenished with an equal volume of fresh buffer medium. The concentration of BSA in collected release samples was measured using Bradford protein assay technique [34], absorbance was measured at 595 nm using a UV–visible spectrophotometer. Each sample was examined in triplicate.

2.5. Mechanical properties

Compressive mechanical properties were analyzed at room temperature on a dynamometric machine (Instron) equipped with a 10 kN load cell and requiring a crosshead speed of 1 mm/min. Tubular-shaped scaffolds (with a diameter of 10 mm) with three different porosities were tested. The force F (kN) and extension (mm) values were recorded throughout the tests. In addition, the apparent stress and strain values were calculated to plot the stress-strain curve for each scaffold. Moreover, the elastic compressive moduli were estimated using the initial linear region of the plotted stress-strain curve.

2.6. Hydrophilicity of the scaffolds

Hydrophilicity is an important parameter of scaffolds for cell attachment and proliferation in cartilage tissue engineering. The water contact angle (WCA) was measured for the scaffolds by Dino-Lite digital microscope analyzer. Distilled water droplets (10 μl) were carefully dropped onto the surface of the specimen. The images of water contact angles were recorded by a microscope camera at 0 s and 20 s after the droplets touched the surface of the scaffold. To determine the water contact angle of each scaffold, three different parts were selected at the ambient temperature and the measurements were performed 8 times.

2.7. In vitro cell study

Human fibroblast cells were used to evaluate the biocompatibility of the 3D fibrous scaffolds. Cells were cultured in DMEM (Gibco) supplemented with 10% FBS (Gibco) and 1% Pen/Strep (Gibco) and harvested at passage 2. The scaffolds were placed in 24-well tissue culture plate and numbers of 100,000 cells were added to each scaffold. The scaffolds were sterilized before use by soaking in 70% ethanol followed by several washes with PBS. For this experiment, the scaffold composed of 15% PCL/CF and DMF were used. The scaffolds were immersed in culture medium one day prior to cell seeding. Cells cultured in tissue culture plate (TCP) were considered as control. The plates incubated at 37 °C and 5% CO_2, and the medium was changed every 2 days. Cell viability was assessed using 3-[4,5-dimethylthiazol-2-yl]-2,5-diphenyl tetrazolium bromide (MTT) assay according to the manufacturer's protocol at day 3 and 7. The metabolic reduction of MTT to a colored formazan by viable cell was measured at 560 nm using a spectrophotometer (BioTek, USA). The percentage viability is expressed as: O.D. of cells in scaffold / O.D of control ∗ 100.

The cells cultured on scaffolds were shown also by FESEM image at day 3. The cell seeded scaffolds were washed two times with PBS and immersed in 10% formalin. After 1 h, the scaffolds were washed with PBS and dehydrated using series ethanol. The samples were dried at room temperature, sputter coated with gold, and imaged by TeScan – Mira III FESEM.

2.8. Statistical analysis

Each experiment was performed in triplicate unless otherwise specified. The results are presented as mean ± standard deviation (SD). Experimental data were analyzed for statistical significance using a one-way analysis of variance (ANOVA) with Turkey's post hoc analysis.

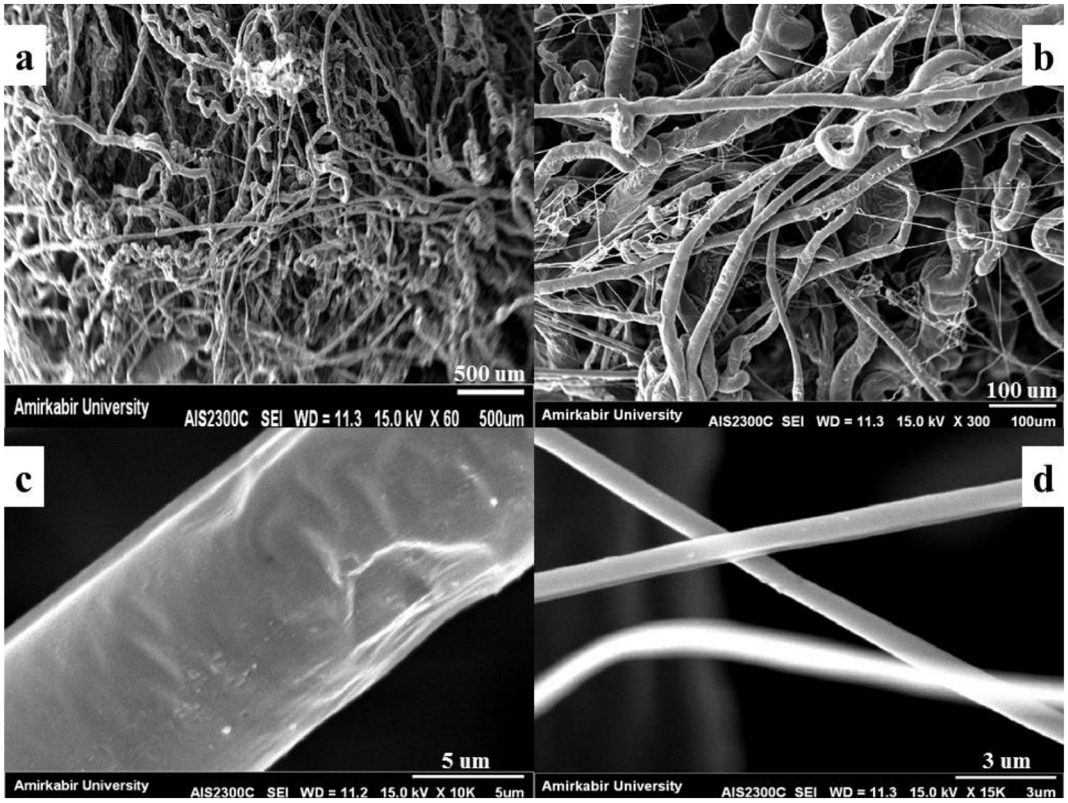

Fig. 3. SEM images of 3-D micro and nanofibrous 6-BSA scaffold prepared by coaxial electrospinning technique. Scale bars are a) 500 μm, b) 100 μm, c) 5 μm, and d) 3 μm.

Statistical significance was set to *p-value < 0.05, **p-value < 0.01, and***p-value < 0.001.

3. Results and discussion

3.1. Characterization of electrospun scaffolds

In coaxial electrospinning, two solutions (e.g. the polymer and protein solutions) were simultaneously electrospun through a coaxial syringe to generate fibers with a core-shell structure. During this process, due to electrostatic forces, surface charges only occurred on the outer solution, therefore the inner solution was not electrospun independently, so it had to rely on the tension of the outer solution to form a complex jet first, and thereafter core-shell structured fibers were formed with the evaporation of shell solvent [35]. Hence, one of the critical parameters for a beadless electrospinning is the flow rate ratio between shell and core.

In this study, the 3D electrospun scaffold was fabricated with wet electrospinning method that is totally different with the structure of 2D scaffolds. Four different SEM images were shown in Fig. 3 to illustrate the nano-micro structures and also the porosity of the 3D scaffold. The SEM images of a selected scaffold (6-BSA) showed relatively uniform fiber morphology with no beads. The structure consists of micro and nanofibers with large pore sizes (Fig. 3). The average fiber diameters for 6-BSA sample was 8 ± 1.6 μm and the average pore size of SEM images were 105 ± 90 μm. The relatively large diameters of the electrospun fibers might be attributed to the high viscosity of the PCL solution, gauge of the coaxial needle and the applied voltage. More SEM images were added to the supplementary.

Based on multiple experiments (which are not included in this manuscript), the optimum flow rate ratio of inner to outer flow was determined at 1:3. So the inner solution could be fully encapsulated by the outer without any dropping, while a stable cone-jet was formed during the whole process.

The porosity of the 3-D scaffolds could be controlled by the density of the scaffold, thus by parameters in the compression of the scaffolds. Three different values of porosity for scaffolds were obtained with shape parameters that are presented in Table 2.

Fig. 4. shows the TEM images of the fibers. Actually, in TEM image different grey levels can be defined as the difference in the electron densities in image plane [37]. The coaxially electrospun scaffolds exhibited an obvious core–shell structure for 6-BSA scaffold, indicated by the differences in electron density between the inner core and outer shell of the fibers. Therefore, in the coaxial electrospinning the drugs or proteins (BSA in this study) can be incorporated in the core part of fibers to have a desirable delivery of bioactive agents and sustained release of them.

In general, PCL coagulates when it is in contact with water that strongly depends on the polymer concentration and temperature [36]. However, in core-shell fibers, the whole PCL is not in contact with water of the core, and the volume ratio of the core water to the polymer solution is 1/3 which is not sufficient for coagulation. Moreover, the core-shell fibers are dehydrated in ethanol bath immediately after spinning. TEM image (Fig. 4) also showed the hollow core of the fibers clearly.

Table 2
Production of different 3D-scaffolds from 6-BSA with different porosities.

Sample	Apparent density ($g/cm^{3)}$	Shape parameters	Porosity
6-BSA	0.370 ± 0.024	D = 10 mm, h = 1 mm	70 ± 2.3%
6-BSA	0.184 ± 0.109	D = 10 mm, h = 2 mm	85 ± 1.08%
6-BSA	0.0807 ± 0.014	D = 10 mm, h = 7 mm	95 ± 2.05%

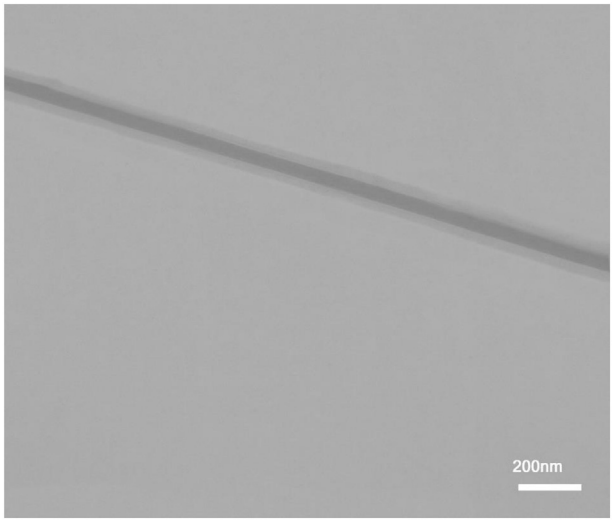

Fig. 4. TEM images of a coaxial fiber of 6-BSA scaffold. The core shell structure was shown in different grey level. Scale bar is 200 nm.

3.2. In vitro BSA release

Fig. 5 shows the cumulative protein release profile from the matrix structure scaffold, with different polymer contents (1-BSA, 2-BSA, and 3-BSA). For all three groups, an initial burst release followed by the slow release rate of BSA. As the polymer content in the fiber increases, BSA release rate decreases.

Compared with coaxial electrospinning, blend electrospinning is easier to perform, nonetheless biomolecules (e.g., proteins) may lose their bioactivity because of structural changes induced by the organic solvent. As coaxial electrospinning utilizes separate channels for the two solutions (i.e. the organic polymer and aqueous biological solutions) it was postulated to be beneficial in maintaining the functional activity of biomolecules. Though, it may not be straightforward to set the parameters which guarantee a stable coaxial electrospinning in order to form a uniform fibrous structure due to differences in the conductivities and viscosities of the two solutions. (Fig. 6).

Fig. 7 shows the cumulative protein release profile from the core-shell structure scaffolds with different polymer contents, (4-BSA, 5-BSA, and 6-BSA). For all three groups, an initial burst release was observed. BSA release was significantly affected by the initial concentration of PCL in the shell solution. The release approached 100%, 91.31%, 72.5% for 10% PCL, 12% PCL, 15% PCL scaffolds, respectively, in 12 days. As expected, by increasing the polymer content in the shell, BSA release rate decreases.

The results showed different protein release profiles from various types of BSA loaded electrospun scaffolds. The burst release may be related to the migration of BSA during dehydration to the fiber surface [38]. When the loaded scaffolds are located in the aqueous environment, the high solubility of BSA may lead to rapid release [39]. After the burst release stage, the core-shell electrospun scaffolds (4-BSA, 5-BSA, and 6-BSA) showed a more sustained release in comparison to the blended fiber scaffolds (1-BSA, 2-BSA, and 3-BSA).

Rapid initial release or burst release is attributed to the fraction of the drug which is adsorbed or weakly bound to the large surface area of the polymer fibers rather than to the drug incorporated into the polymer fibers. The post-release SEM images from 6-BSA (Fig. 8) illustrated the morphological changes in the electrospun fibers after 21 days of BSA release. As shown, the fibers in the coaxial electrospinning scaffold shrunk with respect to their previously smooth cylindrical shape. The average diameters of the fibers in 6-BSA scaffold were measured at day 1 and day 21 post release based on SEM images using Image J software. It was shown that the average fiber diameter decreased from 8 ± 2 μm to 3.5 ± 2 μm from day 1 to 21 which confirms the shrinkage of the fibers during time. The shrinkage of the hollow fibers during time was also shown in previous studies by Jiang et al. [25]. The SEM image of fibers post release with lower magnification was provided in supplementary information.

Fig. 9 compares the cumulative protein release profile from the scaffolds with different structures being matrix (3-BSA) and core-shell

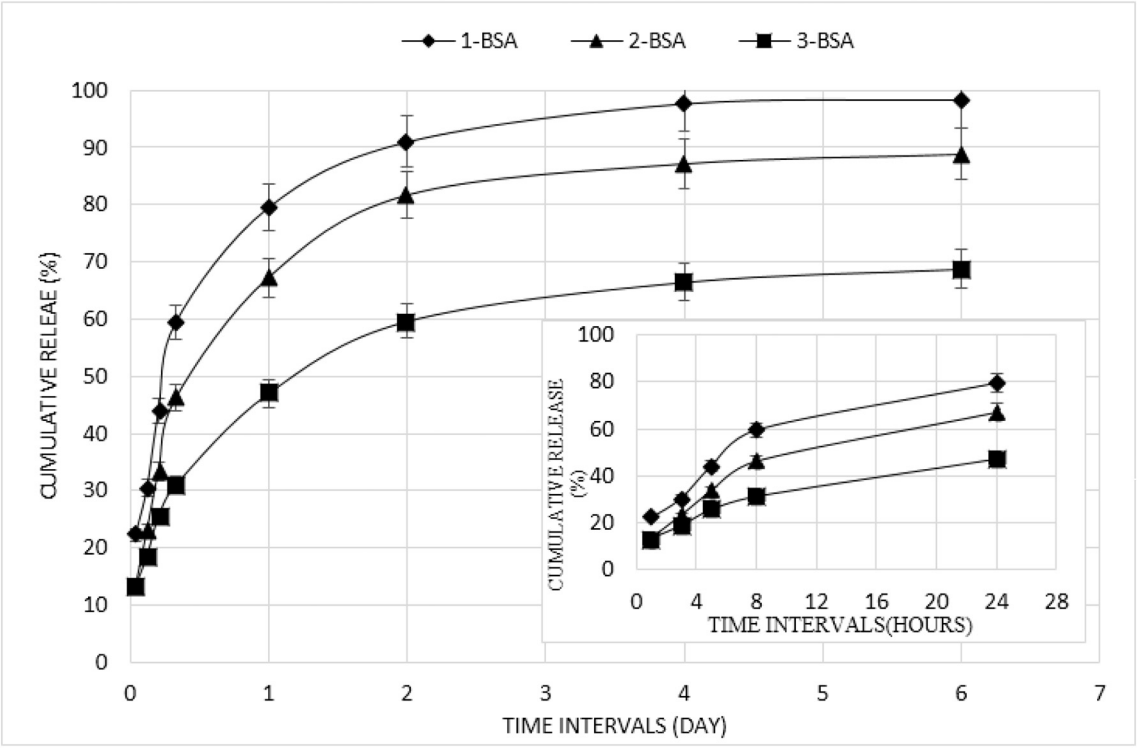

Fig. 5. Cumulative release profile of BSA protein from electrospun scaffolds when BSA was blended in the polymer solution. The amount of loaded BSA is 2% w/w.

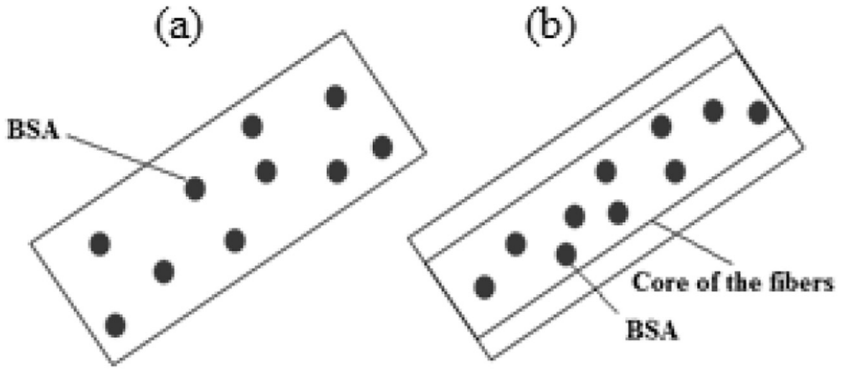

Fig. 6. Schematic of a) matrix structure and b) core-shell structure.

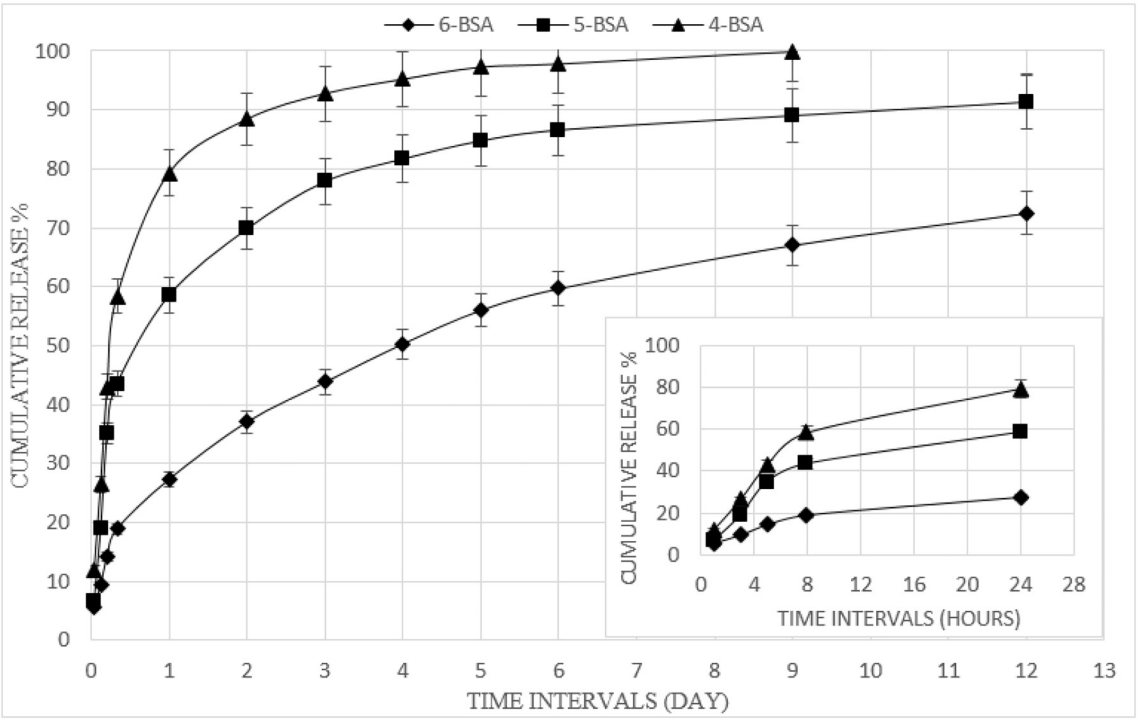

Fig. 7. Cumulative release profile of BSA protein from core-shell electrospun scaffolds when BSA was loaded in the fiber core. The amount of loaded BSA is 2% w/w.

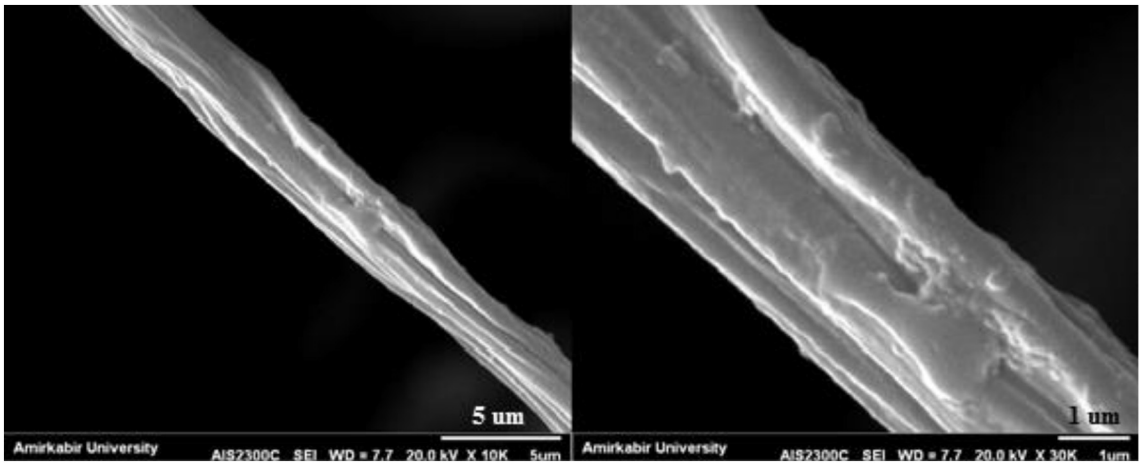

Fig. 8. SEM image of the coaxial electrospun scaffold with BSA incorporation after release study. Scale bars are 5 μm (left) and 1 μm (right).

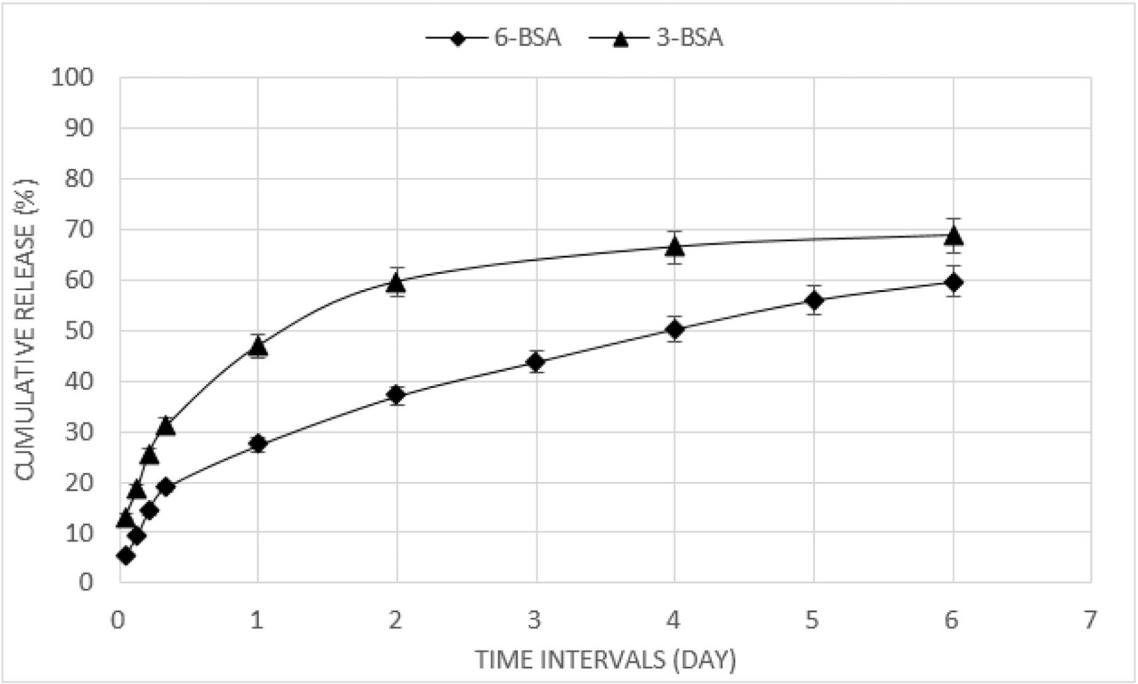

Fig. 9. Cumulative release profile of BSA from matrix (3-BSA) and core-shell (6-BSA) structure system with the same polymer concentration (15% w/v of PCL/CF& DMF) and operating conditions.

(6-BSA). An initial burst release was compared within 8 h, which was 19% and 31% for the core-shell and matrix structure, respectively. In this study, the burst release of BSA from 3-BSA scaffold, in which the protein was mixed in the polymer solution, was about 45%, while the initial burst release from 6-BSA scaffold with core-shell fibers was about 25%. Beside lower burst release of proteins from 6-BSA scaffold, more sustained release was achieved in comparison to 3-BSA construct. The presented results revealed that the release profile of BSA is significantly influenced by structure of the fibers. The protein release rate from the matrix scaffold is higher than that from the core-shell scaffold.

Fig. 10 shows the cumulative protein release profile from the core-shell structure scaffolds with different core flow rates (6-BSA and 7-BSA). This figure revealed that the release profile of BSA is significantly influenced by core flow rate of the fibers. As core flow rate is increased, the loading efficiency increases. Hence, scaffold with the flow rate ratio of 3:1 showed more controllable manner for BSA release in compare with the scaffold with the flow rate ratio of 3:0.5.

3.3. Mechanical properties of 3-D coaxial electrospun scaffolds

Mechanical properties of tissue engineered scaffolds are crucial for in cartilage regeneration. The peak force burdened to knee cartilage during normal physiological loading ranges from 1.9 to 7.2 times body weight [40], which corresponds to approximately 0.84 to 3 MPa for an average person (70 kg). In this study, 3-D electrospun scaffolds with various densities and porosities based on different compaction conditions were characterized. Compressive Young's modulus was determined as slope of the linear region (up to 20% strain) in a stress-strain curve. The average compressive Young's modulus of electrospun scaffolds with different porosities are shown in Table 3. By increasing the compaction forces for making scaffolds, the Young's modulus of the construct increases. This is in accordance with decrease in the pore sizes. Essentially, the cartilage defect size and position guides the characteristics of the proper scaffold for the practice. Accordingly, different characterized scaffolds may be fabricated with customizable mechanical properties to meet the clinical demands.

3.4. Analysis of scaffold hydrophilicity

The surface hydrophilicity of the electrospun fibers plays a dominant role in determining a scaffold as a drug delivery vehicle or a tissue engineering scaffold [41]. Water contact angle analysis is a conventional method to examine the hydrophilicity of fibrous scaffolds. As it is shown in Fig. 11, WCA of 3-D 6-BSA scaffold with 80% porosity is $72.90 \pm 1.12^{\circ}$ at $t = 0$ s and $61.02 \pm 1.04^{\circ}$ at $t = 20$ s, which implies that these 3-D scaffolds, have attained an appropriate hydrophilicity in contrast to traditional 2-D PCL scaffolds with WCA of $> 100^{\circ}$ reported in previous peer-reviewed studies [42,43]. To confirm that the observed hydrophilicity does not relate to the loaded BSA, the WCA was measured for unloaded scaffolds as well. The results of WCA for loaded and unloaded scaffolds were the same as the amounts of $72.90 \pm 1.12^{\circ}$ at $t = 0$ s and $61.02 \pm 1.04^{\circ}$ at $t = 20$ s. Although BSA can increase the hydrophilicity of the structure, here because the protein is loaded in the fiber core, the difference in the WCA amount of loaded and unloaded scaffold was not detected.

3.5. Cell viability

Fig. 12 shows the results of MTT assay at day 3 and 7 after cell seeding on 3D PCL scaffold. The percentage of cell viability (compared to cells cultured in TCP) is 81% and 100% at day 3 and 7, respectively which showed the construct non-toxic. The increase of cell viability from day 3 to day 7 may be attributed to the cell proliferation on the scaffolds during time. The FESEM image of seeded cells on the PCL scaffold is shown in Fig. 12–b & cafter 3 days of culture. The attachment of cells on the scaffold fibers confirmed that the produced structure is biocompatible which is in accordance with the MTT results.

4. Conclusion

Protein-loaded 3-D electrospun scaffolds were prepared using blend and coaxial wet electrospinning techniques for cartilage tissue engineering. Morphologically, these 3-D scaffolds exhibited a uniform fiber structure with suitable pore size. The 3-D tablet-like scaffolds were

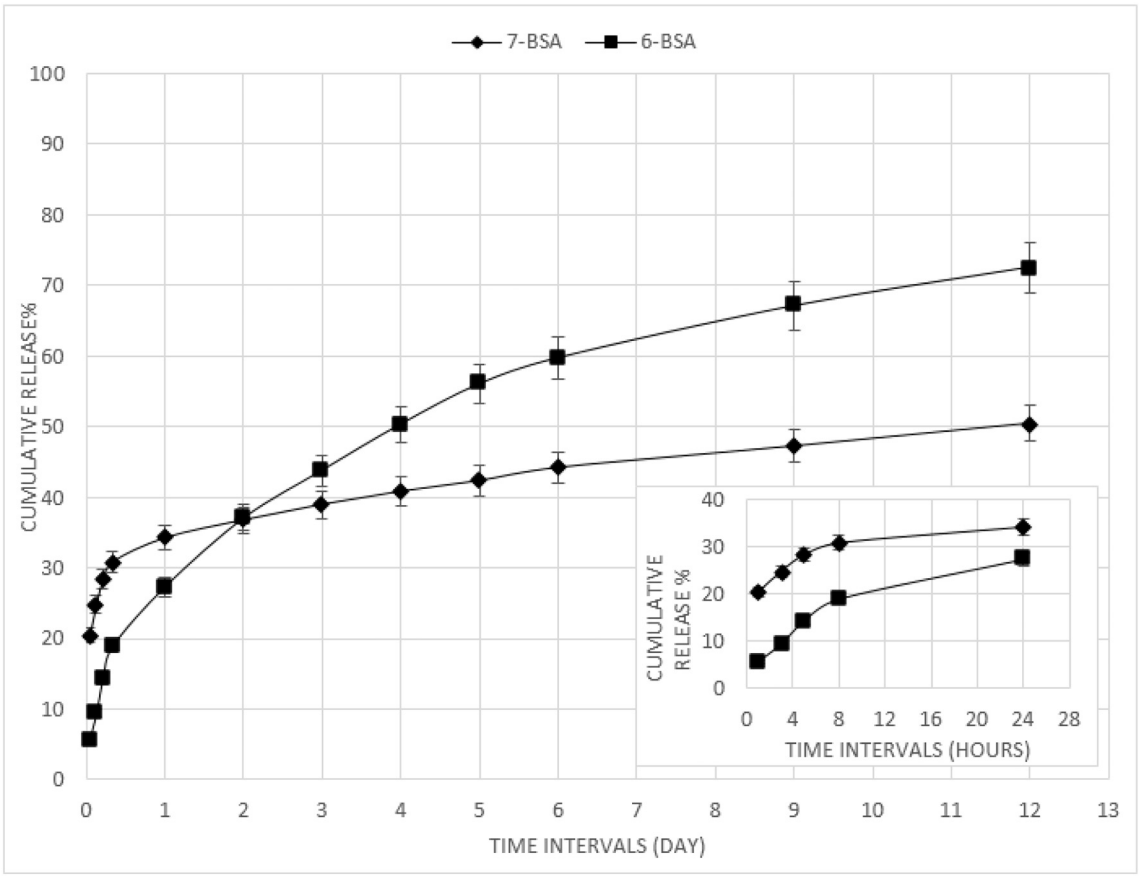

Fig. 10. Cumulative release profile of BSA protein from coaxial electrospun scaffolds. The core flow rate for 6-BSA and 7-BSA scaffolds are 1 and 0.5 mL/h, respectively.

Table 3
Compressive Young's modulus versus porosity of the 3-D scaffold for three different samples.

Sample	Porosity (%)	Young's modulus (MPa)
1-BSA	70 ± 2.3	5 ± 0.68
2-BSA	85 ± 1.05	1.5 ± 0.42
3-BSA	95 ± 2.05	0.3 ± 0.08

expectedly superior to the conventional 2-D PCL scaffolds with respect to porosity and hydrophilicity for cell attachment and proliferation. Dictated by the cartilage defect size and position, scaffolds with customized size and porosity could be constructed with desirable mechanical properties proportionate to the native tissue demands. The release profiles of BSA from different scaffolds were evaluated and compared. The coaxial scaffolds showed more sustained release profiles in comparison to their counterpart blend scaffolds. Moreover, the in vitro cell cytotoxicity assay revealed that the constructed scaffold was biocompatible and non-toxic. Therefore, coaxial electrospinning represents a promising method for protein incorporation with preservation of biological activity of the loaded protein in the scaffolds. These protein loaded 3-D PCL scaffolds may serve as an appropriate controlled release engineered system for cartilage regeneration.

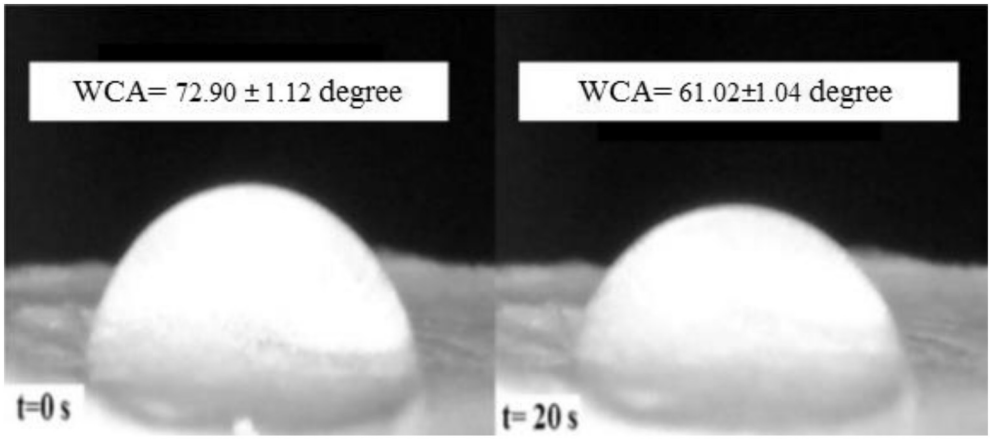

Fig. 11. WCA of 6-BSA scaffolds from 0 s to 20 s.

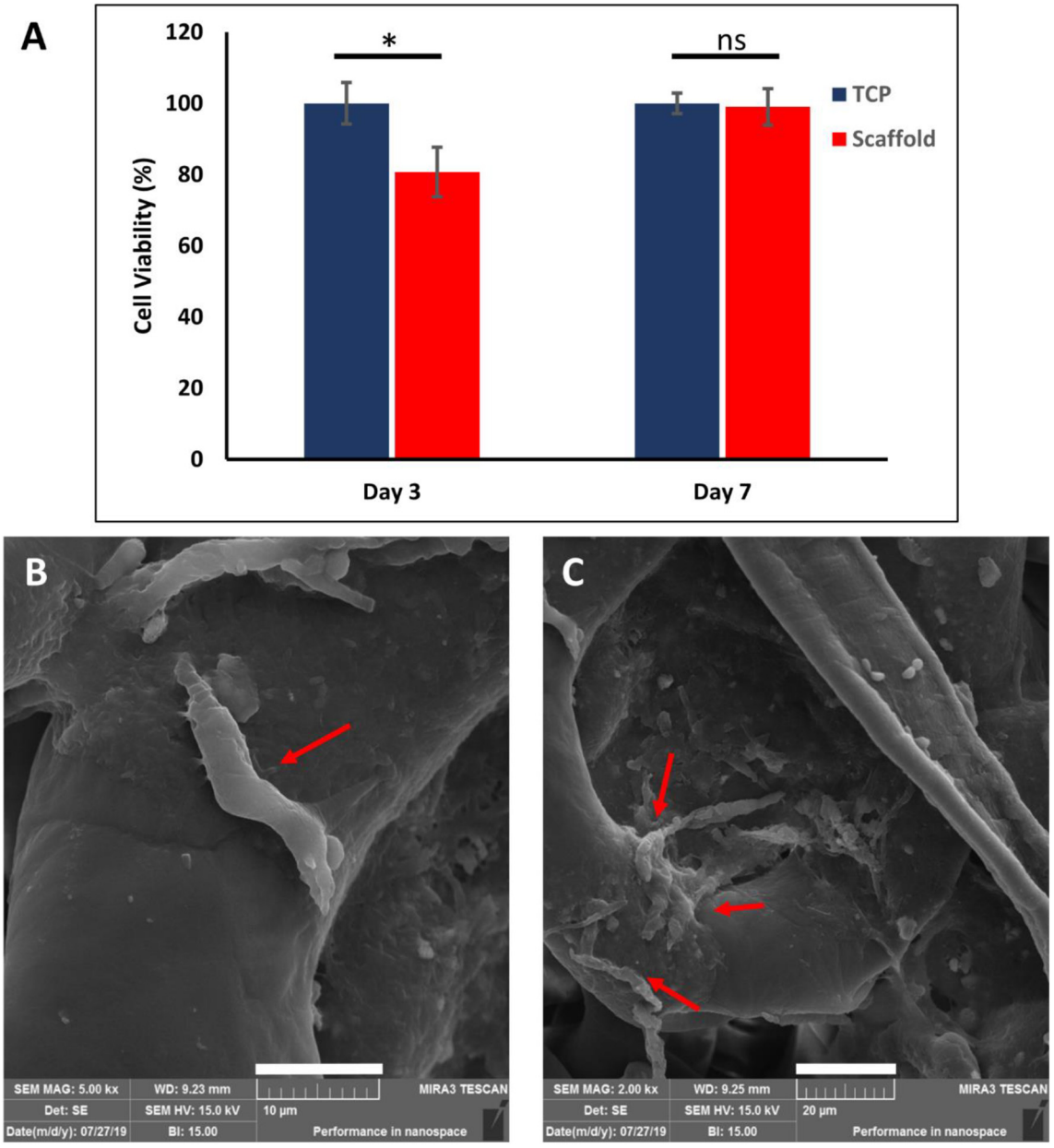

Fig. 12. Interaction of cells with 3D PCL scaffold. a) MTT assay of Fibroblast cells cultured on the PCL scaffold. Error bars were mean ± SD ($n = 3$; *p < 0.05, ns: not significant). b, c) SEM images of cultured cells on the electrospun scaffold. The cells were shown with arrows. Scale bars are 10 and 20 µm, respectively.

CRediT authorship contribution statement

Mehrnoosh Rafiei: Conceptualization, Methodology, Investigation, Writing - original draft, Visualization, Validation.**Elaheh Jooybar:**Writing - review & editing, Supervision, Funding acquisition.**Mohammad J. Abdekhodaie:**Writing - review & editing, Supervision.**Mansour Alvi:**Writing - review & editing.

Declaration of competing interest

The authors declare that they have no known competing financial interests or personal relationships that could have appeared to influence the work reported in this paper.

Acknowledgements

The authors wish to thank Iran National Science Foundation (INSF) under grant number 94004082 for supporting this project.

Appendix A. Supplementary data

Supplementary data to this article can be found online at https://doi.org/10.1016/j.msec.2020.110913.

References

[1] R. Tuli, W.-J. Li, R.S. Tuan, Current state of cartilage tissue engineering, Arthritis Res. Ther. 5 (5) (2003) 1.
[2] M.L. Alves da Silva, A. Martins, A.R. Costa-Pinto, P. Costa, S. Faria, M. Gomes, et al., Cartilage tissue engineering using electrospun PCL nanofiber meshes and MSCs, Biomacromolecules 11 (12) (2010) 3228–3236.
[3] A.M. Bhosale, J.B. Richardson, Articular cartilage: structure, injuries and review of management, Br. Med. Bull. 87 (1) (2008) 77–95.
[4] E.J. Caterson, L.J. Nesti, W.J. Li, K.G. Danielson, T.J. Albert, A.R. Vaccaro, et al., Three-dimensional cartilage formation by bone marrow-derived cells seeded in polylactide/alginate amalgam, J. Biomed. Mater. Res. 57 (3) (2001) 394–403.
[5] C. Chung, J.A. Burdick, Engineering cartilage tissue, Adv. Drug Deliv. Rev. 60 (2)

(2008) 243–262.
[6] M. Demoor, D. Ollitrault, T. Gomez-Leduc, M. Bouyoucef, M. Hervieu, H. Fabre, et al., Cartilage tissue engineering: molecular control of chondrocyte differentiation for proper cartilage matrix reconstruction, Biochim. Biophys. Acta Gen. Subj. 1840 (8) (2014) 2414–2440.
[7] Y. Yang, T. Zhu, Z. Liu, M. Luo, D.-G. Yu, S.A. Bligh, The key role of straight fluid jet in predicting the drug dissolution from electrospun nanofibers, Int. J. Pharm. 569 (2019) 118634.
[8] Q. Wang, D.-G. Yu, L.-L. Zhang, X.-K. Liu, Y.-C. Deng, M. Zhao, Electrospun hypromellose-based hydrophilic composites for rapid dissolution of poorly water-soluble drug, Carbohydr. Polym. 174 (2017) 617–625.
[9] M. Wang, T. Hai, Z. Feng, D.-G. Yu, Y. Yang, S. Annie Bligh, The relationships between the working fluids, process characteristics and products from the modified coaxial electrospinning of zein, Polymers 11 (8) (2019) 1287.
[10] K. Wang, X.-K. Liu, X.-H. Chen, D.-G. Yu, Y.-Y. Yang, P. Liu, Electrospun hydrophilic Janus nanocomposites for the rapid onset of therapeutic action of helicid, ACS Appl. Mater. Interfaces 10 (3) (2018) 2859–2867.
[11] Z. Gong, Y. Du, Y. He, A. Yang, Y. Yang, D. Yu, The Influence of DMAc Ratio in Sheath Fluid on the Diameters of Medicated Cellulose Acetate Nanofibers, (2019).
[12] G.-Z. Yang, J.-J. Li, D.-G. Yu, M.-F. He, J.-H. Yang, G.R. Williams, Nanosized sustained-release drug depots fabricated using modified tri-axial electrospinning, Acta Biomater. 53 (2017) 233–241.
[13] D.-G. Yu, J.-J. Li, M. Zhang, G.R. Williams, High-quality Janus nanofibers prepared using three-fluid electrospinning, Chem. Commun. 53 (33) (2017) 4542–4545.
[14] J. Rnjak-Kovacina, A.S. Weiss, Increasing the pore size of electrospun scaffolds, Tissue Eng. B Rev. 17 (5) (2011) 365–372.
[15] S. Zhong, Y. Zhang, C.T. Lim, Fabrication of large pores in electrospun nanofibrous scaffolds for cellular infiltration: a review, Tissue Eng. B Rev. 18 (2) (2012) 77–87.
[16] Y. Yokoyama, S. Hattori, C. Yoshikawa, Y. Yasuda, H. Koyama, T. Takato, et al., Novel wet electrospinning system for fabrication of spongiform nanofiber 3-dimensional fabric, Mater. Lett. 63 (9) (2009) 754–756.
[17] T.G. Kim, D.S. Lee, T.G. Park, Controlled protein release from electrospun biodegradable fiber mesh composed of poly (ε-caprolactone) and poly (ethylene oxide), Int. J. Pharm. 338 (1) (2007) 276–283.
[18] H. Zhou, Z. Shi, X. Wan, H. Fang, D.-G. Yu, X. Chen, et al., The relationships between process parameters and polymeric nanofibers fabricated using a modified coaxial electrospinning, Nanomaterials 9 (6) (2019) 843.
[19] W. Ji, F. Yang, J.J. Van den Beucken, Z. Bian, M. Fan, Z. Chen, et al., Fibrous scaffolds loaded with protein prepared by blend or coaxial electrospinning, Acta Biomater. 6 (11) (2010) 4199–4207.
[20] Y. Li, H. Jiang, K. Zhu, Encapsulation and controlled release of lysozyme from electrospun poly (ε-caprolactone)/poly (ethylene glycol) non-woven membranes by formation of lysozyme–oleate complexes, J. Mater. Sci. Mater. Med. 19 (2) (2008) 827–832.
[21] S. Puhl, L. Li, L. Meinel, O. Germershaus, Controlled protein delivery from electrospun non-wovens: novel combination of protein crystals and a biodegradable release matrix, Mol. Pharm. 11 (7) (2014) 2372–2380.
[22] S. Srouji, D. Ben-David, R. Lotan, E. Livne, R. Avrahami, E. Zussman, Slow-release human recombinant bone morphogenetic protein-2 embedded within electrospun scaffolds for regeneration of bone defect: in vitro and in vivo evaluation, Tissue Eng. A 17 (3–4) (2010) 269–277.
[23] I. Liao, S. Chew, K. Leong, Aligned core–shell nanofibers delivering bioactive proteins, Nanomedicine 1 (4) (2006) 465–471.
[24] L. Li, G. Zhou, Y. Wang, G. Yang, S. Ding, S. Zhou, Controlled dual delivery of BMP-2 and dexamethasone by nanoparticle-embedded electrospun nanofibers for the efficient repair of critical-sized rat calvarial defect, Biomaterials 37 (2015) 218–229.
[25] H. Jiang, Y. Hu, Y. Li, P. Zhao, K. Zhu, W. Chen, A facile technique to prepare biodegradable coaxial electrospun nanofibers for controlled release of bioactive agents, J. Control. Release 108 (2) (2005) 237–243.
[26] H. Jiang, Y. Hu, P. Zhao, Y. Li, K. Zhu, Modulation of protein release from biodegradable core–shell structured fibers prepared by coaxial electrospinning, J Biomed Mater Res B Appl Biomater 79 (1) (2006) 50–57.
[27] Y. Su, X. Li, Y. Liu, Q. Su, M.L.W. Qiang, X. Mo, Encapsulation and controlled release of heparin from electrospun poly (l-lactide-co-ε-caprolactone) nanofibers, J. Biomater. Sci. Polym. Ed. 22 (1–3) (2011) 165–177.
[28] M. Rubert, J. Dehli, Y.-F. Li, M.B. Taskin, R. Xu, F. Besenbacher, et al., Electrospun PCL/PEO coaxial fibers for basic fibroblast growth factor delivery, J. Mater. Chem. B 2 (48) (2014) 8538–8546.
[29] M. Buzgo, R. Jakubova, A. Mickova, M. Rampichova, E. Prosecka, P. Kochova, et al., Time-regulated drug delivery system based on coaxially incorporated platelet α-granules for biomedical use, Nanomedicine 8 (7) (2013) 1137–1154.
[30] L. Ghasemi-Mobarakeh, D. Semnani, M. Morshed, A novel method for porosity measurement of various surface layers of nanofibers mat using image analysis for tissue engineering applications, J. Appl. Polym. Sci. 106 (4) (2007) 2536–2542.
[31] D. Han, S.T. Boyce, A.J. Steckl (Eds.), Versatile Core-Sheath Biofibers Using Coaxial Electrospinning, Cambridge Univ Press, MRS Proceedings, 2008.
[32] H. Lee, M. Yeo, S. Ahn, D.O. Kang, C.H. Jang, H. Lee, et al., Designed hybrid scaffolds consisting of polycaprolactone microstrands and electrospun collagen-nanofibers for bone tissue regeneration, J Biomed Mater Res B Appl Biomater 97 (2) (2011) 263–270.
[33] A. Szentivanyi, T. Chakradeo, H. Zernetsch, B. Glasmacher, Electrospun cellular microenvironments: understanding controlled release and scaffold structure, Adv. Drug Deliv. Rev. 63 (4) (2011) 209–220.
[34] N. Krüger, J. WALKER, The Bradford Method for Protein Quantification. The Protein Protocols Handbook, 2nd edition, Humana Press Inc, New Jersey, 2002, pp. 15–22.
[35] M. Graeser, M. Bognitzki, W. Massa, C. Pietzonka, A. Greiner, J.H. Wendorff, Magnetically anisotropic cobalt and iron nanofibers via electrospinning, Adv. Mater. 19 (23) (2007) 4244–4247.
[36] D. Puppi, A.M. Piras, F. Chiellini, E. Chiellini, A. Martins, I.B. Leonor, et al., Optimized electro-and wet-spinning techniques for the production of polymeric fibrous scaffolds loaded with bisphosphonate and hydroxyapatite, J. Tissue Eng. Regen. Med. 5 (4) (2011) 253–263.
[37] L. Reimer, Transmission Electron Microscopy: Physics of Image Formation and Microanalysis, Springer, 2013.
[38] S.D. Allison, Analysis of initial burst in PLGA microparticles, Expert Opin. Drug Deliv. 5 (6) (2008) 615–628.
[39] X. Huang, C.S. Brazel, On the importance and mechanisms of burst release in matrix-controlled drug delivery systems, J. Control. Release 73 (2–3) (2001) 121–136.
[40] Z. Izadifar, X. Chen, W. Kulyk, Strategic design and fabrication of engineered scaffolds for articular cartilage repair, J. Funct. Biomater. 3 (4) (2012) 799–838.
[41] S. Yan, L. Xiaoqiang, L. Shuiping, M. Xiumei, S. Ramakrishna, Controlled release of dual drugs from emulsion electrospun nanofibrous mats, Colloids Surf. B: Biointerfaces 73 (2) (2009) 376–381.
[42] S.-H. Chen, C.-H. Chen, K. Shalumon, J.-P. Chen, Preparation and characterization of antiadhesion barrier film from hyaluronic acid-grafted electrospun poly (caprolactone) nanofibrous membranes for prevention of flexor tendon postoperative peritendinous adhesion, Int. J. Nanomedicine 9 (2014) 4079.
[43] J. Hersey, S. Yohe, M. Grinstaff, Poly (ε-caprolactone) microfiber meshes for repeated oil retrieval, Environ. Sci.: Water Res. Technol. 1 (6) (2015) 779–786.